

This is the accepted manuscript made available via CHORUS. The article has been published as:

The $^{136}\text{Xe} + ^{198}\text{Pt}$ reaction: A test of models of multi-nucleon transfer reactions

V. V. Desai, W. Loveland, K. McCaleb, R. Yanez, G. Lane, S. S. Hota, M. W. Reed, H. Watanabe, S. Zhu, K. Auranen, A. D. Ayangeakaa, M. P. Carpenter, J. P. Greene, F. G. Kondev, D. Seweryniak, R. V. F. Janssens, and P. A. Copp

Phys. Rev. C **99**, 044604 — Published 16 April 2019

DOI: [10.1103/PhysRevC.99.044604](https://doi.org/10.1103/PhysRevC.99.044604)

The $^{136}\text{Xe} + ^{198}\text{Pt}$ reaction: A test of models of multi-nucleon transfer reactions

V. V. Desai, W. Loveland, K. McCaleb, R. Yanez

Department of Chemistry, Oregon State University, Corvallis, Oregon 97331 USA

G. Lane, S.S. Hota, M.W. Reed, H. Watanabe

Australian National University, Canberra, Australia

S. Zhu, K. Auranen, A. D. Ayangeakaa,* and M. P.

Carpenter, J.P. Greene, F. G. Kondev, D. Seweryniak

Physics Division, Argonne National Laboratory, Argonne, Illinois 60439 USA

R.V.F. Janssens

Department of Physics and Astronomy,

University of North Carolina at Chapel Hill, Chapel Hill,

North Carolina 27599 USA and Triangle Universities Nuclear Laboratory,

Duke University, Durham, North Carolina 27708 USA

P.A. Copp

Dept. of Physics, University of Massachusetts Lowell, Lowell MA 01854 USA

Abstract

The yields of 42 projectile-like fragments (PLFs) and fission fragments and 36 target-like fragments (TLFs) were measured using off-line γ -ray spectroscopy in a thin target experiment involving the $^{136}\text{Xe} + ^{198}\text{Pt}$ reaction. The center of target beam energy was 760.5 MeV($E_{c.m.} = 450$ MeV). The reported yields are compared with those from previous measurements for this reaction and with predictions of the GRAZING, di-nuclear systems (DNS) and Improved Quantum Molecular Dynamics (ImQMD)models. The yields of the TLFs and PLFs are, in general, substantially smaller than those previously observed at a beam energy of 1085 MeV. Neither the GRAZING or DNS models correctly describes the measured TLF and PLF yields in this lower- energy reaction but the ImQMD model describes these yields adequately.

* Present address: United States Naval Academy, Annapolis, Maryland 21402 USA

I. INTRODUCTION

Multi-nucleon transfer (MNT) reactions are thought to be useful paths for synthesizing new n-rich heavy nuclei [1, 2] and as possible paths for synthesizing nuclei near the $N=126$ shell closure (of interest to the studies of r-process nucleosynthesis [3]). Watanabe et al. [4] measured the yields of the projectile-like fragments (PLFs) formed in the reaction of $E_{lab} = 7.98$ A MeV ($E_{c.m.} = 4.73$ A MeV) $^{136}\text{Xe} + ^{198}\text{Pt}$. The PLFs were detected around the grazing angle ($\approx 33^\circ$) using the VAMOS++ spectrometer. Absolute cross sections were determined for PLFs ranging from Sn to Ce. Absolute cross sections were also determined for Os and Hg target-like fragments (TLFs). Production cross sections were reported for the $N=126$ isotones W, Re, Os, Ir, and Pt. These results have motivated a number of calculations using various theoretical models for these MNT reactions ([5–7]). In [5] the di-nuclear systems (DNS) model is used to describe the data and the calculated and measured values of the PLF cross sections are in reasonable agreement. In [6] the model used to describe the data was the Improved Quantum Molecular Dynamics (ImQMD) model and there was good agreement between measured and calculated cross sections. Improvements in the DNS model were made and tested in [7] with better agreement between calculations and measurements when compared to [5].

In this work, we measured the yields of various PLFs and TLFs in the interaction of ^{136}Xe with ^{198}Pt at a substantially lower beam energy ($E_{lab} = 760.5$ MeV ($E_{c.m.} = 450$ MeV)) compared to the study of Watanabe [4] where E_{lab} was 1085 MeV. The use of a beam energy of $\approx 1.1 V_B$ where V_B is the Bass barrier [8] is thought by some [3] to be a better choice for making heavy trans-target nuclei. (It should be pointed out, however, that some models [9, 10] predict that the yields of the MNT products are weakly energy dependent.) In any case, the comparison of the lower and higher energy reactions should be useful in testing models for these collisions.

II. EXPERIMENTAL

The experimental method used was similar to that of Barrett et al. [11]. Using the Gammasphere facility of the Argonne National Laboratory, a beam of 860 MeV ^{136}Xe struck a sandwich of a 3.2 mg/cm² ^{198}Pt foil, a 4.0 mg/cm² ^{198}Pt foil and a 24 mg/cm² ^{197}Au stopper foil. The isotopic purity of the ^{198}Pt foils was established in a post-experiment measurement by the W.M. Keck Collaboratory for Plasma Mass Spectrometry [12] to be 95.0 atom percent ^{198}Pt , 2.84 atom percent ^{196}Pt , 1.23 atom percent ^{195}Pt and 0.9 atom percent ^{194}Pt . The mean beam energy in the Pt foil stack was $E_{lab} = 760.5$ MeV. The intensity of the beam was monitored periodically by inserting a suppressed Faraday cup into the beam line in front of the target. The length of the irradiation was 28.3 h with an average beam intensity of 3.54×10^8 p/s.

At the end of the irradiation, the target was removed from Gammasphere and γ -ray spectroscopy of the target radioactivities was carried out using a well-calibrated Ge detector in The Center for Accelerator Target Science (CATS) Counting Laboratory. The total observation period was 5 days, during which 19 measurements of target radioactivity were made. The analysis of these Ge γ -ray decay spectra was carried out using the FitzPeaks [13] software. The end of bombardment (EOB) activities of the nuclides were used to calculate absolute production cross sections, taking into account the variable beam intensities using standard equations for the growth and decay of radionuclides during irradiation [14]. These measured absolute nuclidic production cross sections are tabulated in Table 1 and Table 2. These cross sections represent “cumulative” yields, i.e., they have not been corrected for the effects of precursor beta decay. These cumulative yields are the primary measured quantity in this experiment.

To correct for precursor beta decay, we have assumed that the beta-decay cor-

rected independent yield cross sections for a given species, $\sigma(Z,A)$, can be represented as a histogram that lies along a Gaussian curve

$$\sigma(Z, A) = \sigma(A) [2\pi C_Z^2(A)]^{-1/2} \exp \left[\frac{-(Z - Z_{mp})^2}{2C_Z^2(A)} \right] \quad (1)$$

where $\sigma(A)$ is the total isobaric yield (the mass yield), $C_Z(A)$ is the Gaussian width parameter for mass number A , and $Z_{mp}(A)$ is the most probable atomic number for that A . Given this assumption, the beta-decay feeding correction factors for cumulative yield isobars can be calculated, once the centroid and width of the Gaussian function are known.

To uniquely specify $\sigma(A)$, $C_Z(A)$, and $Z_{mp}(A)$, one would need to measure three independent yield cross sections for each isobar. That does not happen often. Instead one assumes that the value of $\sigma(A)$ varies smoothly and slowly as a function of mass number and is roughly constant within any A range when determining $C_Z(A)$ and $Z_{mp}(A)$. The measured nuclidic formation cross sections are then placed in groups according to mass number. We assume that the charge distributions of neighboring isobaric chains are similar and radionuclide yields from a limited mass region can be used to determine a single charge distribution curve for that mass region. One can then use the laws of radioactive decay to iteratively correct the measured cumulative formation cross sections for precursor decay. These “independent yield” cross sections are also tabulated in Tables 1 and 2. The cumulative and independent yield cross sections are similar due to the fact that, without an external separation of the reaction products by Z or A , one most likely detects only a single or a few nuclides for a given isobaric chain and these nuclides are located near the maximum of the Gaussian yield distribution. The uncertainties in the calculated “independent yield” cross sections deduced in this manner have been examined by Morrissey et al. [15] and they have found a systematic uncertainty of $\pm 30\%$ associated with this procedure.

III. RESULTS AND DISCUSSION

A. This Work

The measured cumulative and independent yields of the projectile-like fragments (PLFs) and target-like fragments (TLFs) from the interaction of $E_{c.m.} = 451$ MeV ^{136}Xe with ^{198}Pt form a large data set (78 yields) to characterize the product distributions from this reaction. The magnitudes of the measured cross sections range from $\approx 70\mu\text{b}$ to ≈ 200 mb. The observed PLFs span the region from $Z=48$ to $Z=71$ (Xe is $Z=54$) while the observed TLFs range from $Z=72$ to $Z=83$ (Pt is $Z = 78$). The observed nuclides are located “north-east” of the projectile and “south-west” of the target although there are several notable exceptions. Unknown nuclei cannot be observed using our experimental methods. No nuclei with $N=126$ were observed in this experiment.

B. Comparison with previous measurements

As mentioned earlier, Watanabe [4] measured the yields of several PLFs in the reaction of 1085 MeV ^{136}Xe with ^{198}Pt . The beam energy in that study was substantially higher than in this work (760.5 MeV). In Figure 1, we compare the yields of several PLFs measured in the two studies. As shown in Figure 1, the measured PLF yields are substantially higher at the higher bombarding energy with the possible exceptions of the yields of ^{135}Xe and ^{140}Ba . We can conclude that the higher bombarding energy leads to increased yields of the PLFs. What about the yields of the TLFs where fission might act to deplete the yields at the higher excitation energies? In Figure 2, we compare the yields of the Hg and Os nuclides measured in this work with those of Watanabe [4]. The same general trends observed for the PLFs are seen

for the TLFs with the exception of ^{203}Hg . This suggests that the higher bombarding energy is more effective than the near barrier energy in producing new transfer products. The increased survival rates at the lower energy do not compensate for the lower yields of the primary products.

C. Comparison with phenomenological models

To compare our measured cross sections with estimates of various phenomenological models (which may differ by orders of magnitude), we define a comparison metric [16], the theory evaluation factor, **t_{ef}**.

For each data point, we define

$$t_{ef_i} = \log \left(\frac{\sigma_{theory}}{\sigma_{expt}} \right) \quad (2)$$

where σ_{theory} and σ_{expt} are the calculated and measured values of the transfer cross sections. Then, the average theory evaluation factor is given by

$$\overline{t_{ef}} = \frac{1}{N_d} \sum_{i=1}^{N_d} t_{ef_i} \quad (3)$$

where N_d is the number of data points. The variance of the average theory evaluation factor is given by

$$\sigma = \frac{1}{N_d} \left(\sum_i (t_{ef_i} - \overline{t_{ef}})^2 \right)^{1/2} \quad (4)$$

Note that **t_{ef}** is a logarithmic quantity and theories that have **t_{ef}** values differing by 1 or 2 actually differ by orders of magnitude in their reliability.

A well-known model for predicting the cross sections for transfer products is GRAZING, a semi-classical model due to Pollaro and Winther [17, 18]. GRAZING uses a semi-classical model of the reacting ions moving on classical trajectories with quantum calculations of the probability of excitation of collective states and of

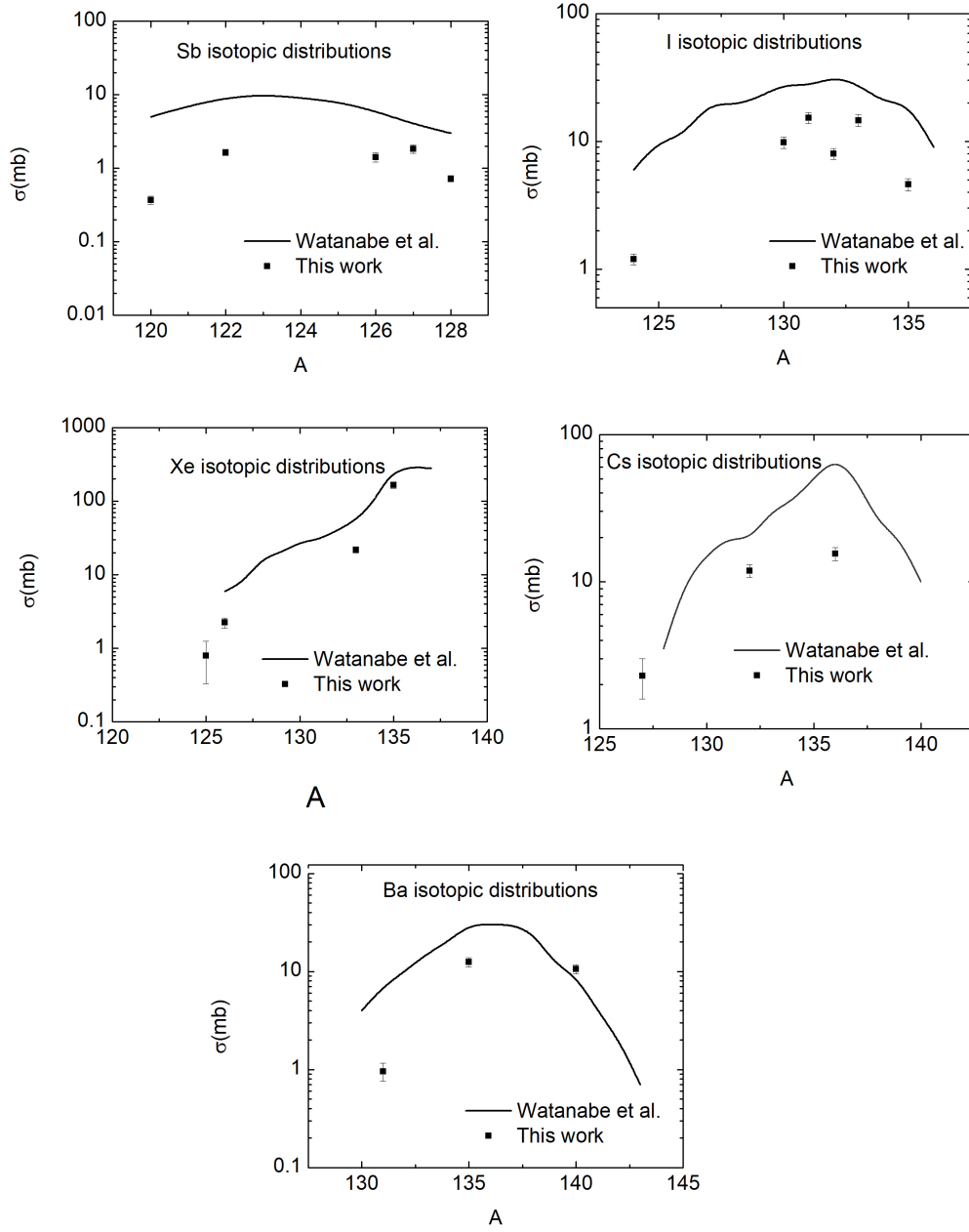


FIG. 1. Comparison of measured PLF yields for the work of Watanabe [4] and this work.

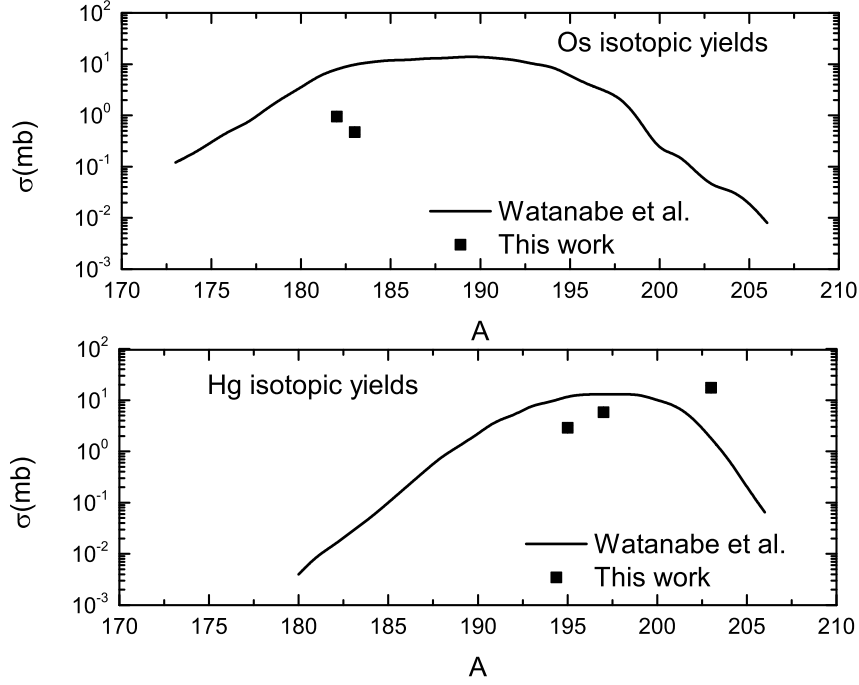


FIG. 2. Comparison of measured TLF yields for the isotopes of Hg and Os studied in the work of Watanabe [4] and this work.

nucleon transfer. This model describes few nucleon transfers [19] well. It has been employed to describe the production of projectile like fragments (PLFs) involving transfers of 45 nucleons in the asymmetric reaction of ^{136}Xe with ^{238}U , where the

predictions of this model agree well with measurements [20]. The measured and predicted (GRAZING) values for the PLF and TLF cross sections are shown in Figures 3 -6.

The GRAZING model correctly predicts the magnitudes of the transfer cross sections for small transfers, but underestimates the cross sections for large transfers. Comparing the measured and calculated (GRAZING) values of the TLF cross sections gives an average **tef** value of -1.353 ± 0.044 , i.e., GRAZING underestimates the TLF yields by a factor of 23, on average.

Another phenomenological model that is frequently used to estimate yields from multi-nucleon transfer reactions is the di-nuclear systems (DNS) model [5, 7]. In Figures 3-6, we compare our measured deduced independent yield cross sections for the $^{136}\text{Xe} + ^{198}\text{Pt}$ reaction with the predictions of the DNS model. For all of the PLF yields, the DNS model significantly underestimates the measured PLF yields. For the TLFs, the DNS model underestimates the magnitude of the MNT cross sections. Comparing the measured and calculated (DNS) values of the TLF cross sections gives an average **tef** values of -1.724 ± 0.211 , i.e, the DNS model underestimates the TLF yields by a factor of 53 on average.

A third phenomenological model whose predictions can be compared to our data is the Improved Quantum Molecular Dynamics (ImQMD) model. Our measured independent MNT product yields are compared to the predictions of the ImQMD model in Figures 3-6. Unlike the GRAZING and DNS models, the predictions of the ImQMD model describe the data for all transfers ($\Delta Z = -5$ to $+17$ for PLFs and $\Delta Z = -6$ to $+6$ for TLFs). Comparing the measured and calculated (ImQMD) values of the TLF cross sections gives an average **tef** value of -0.00893 ± 0.084 , i.e., the ImQMD model mis-estimates the TLF yields by a factor of 0.98 . The ImQMD model is thus superior to the GRAZING and DNS models in its predictive power.

The fragment mass yields represent another test of the theoretical models for

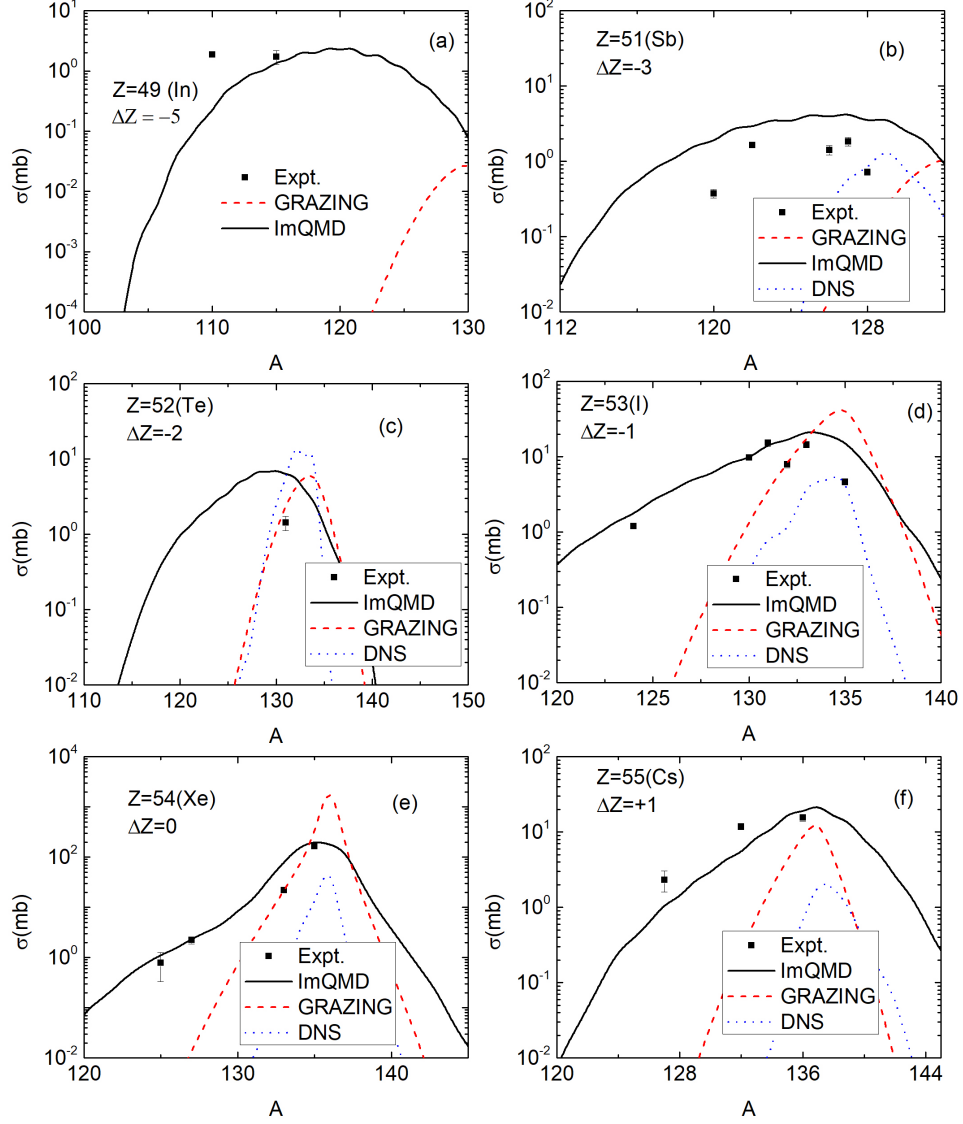


FIG. 3. Comparison of measured PLF (In-Cs) yields to the predictions of the ImQMD, GRAZING and DNS models.

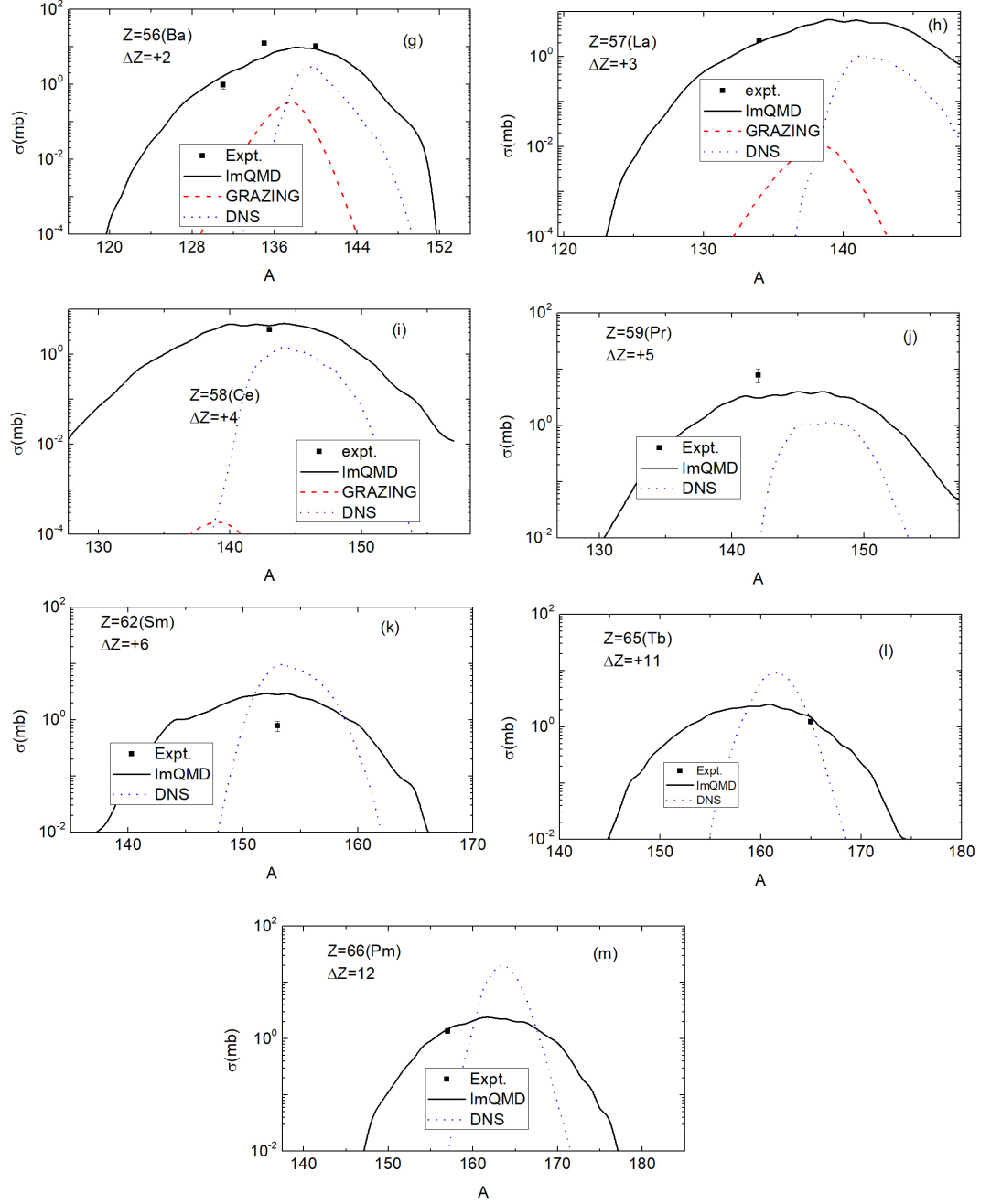


FIG. 4. Comparison of measured PLF (Ba-Pm) yields to the predictions of the ImQMD, GRAZING and DNS models.

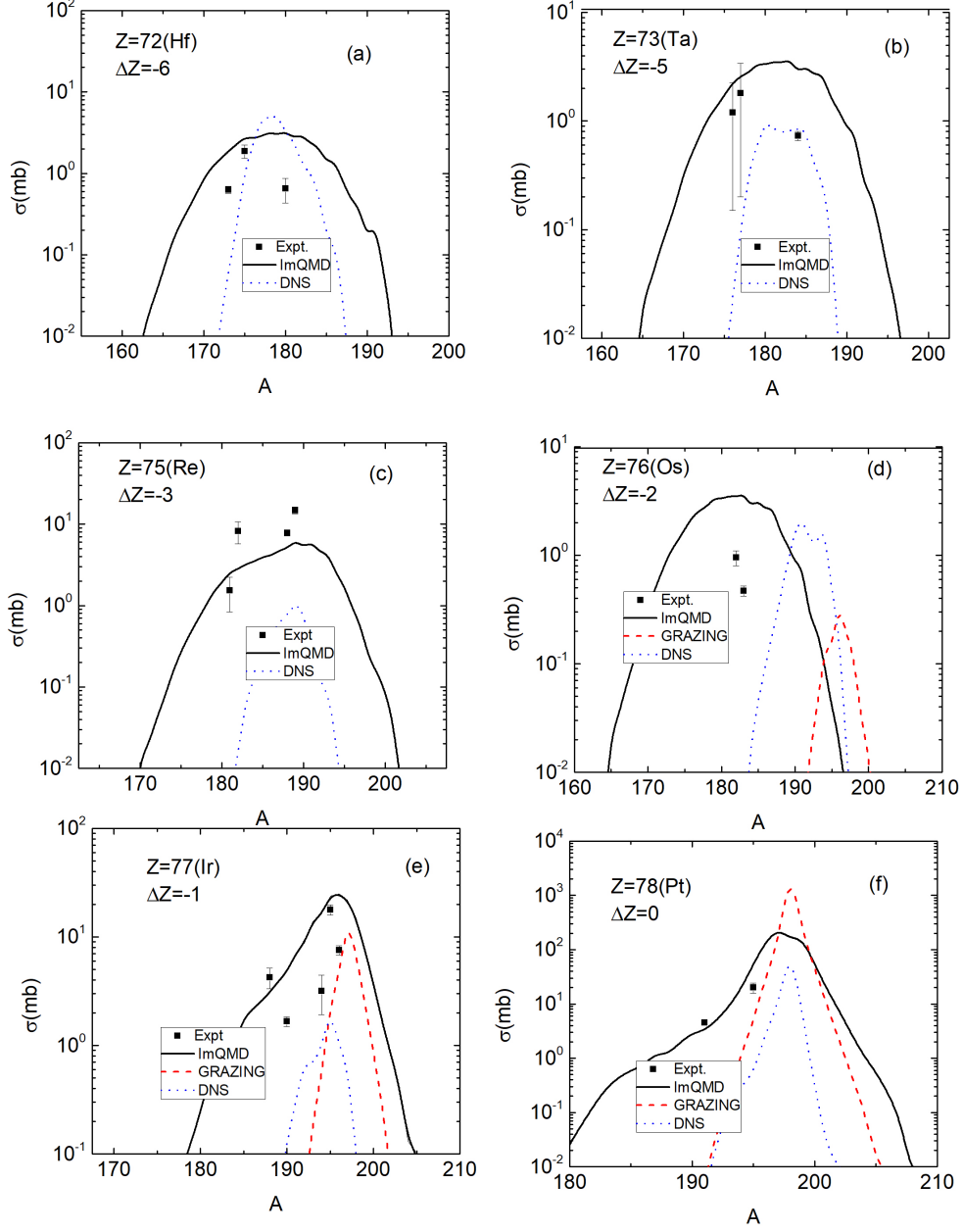


FIG. 5. Comparison of measured TLF yields (Hf-Pt) to the predictions of the ImQMD, GRAZING and DNS models.

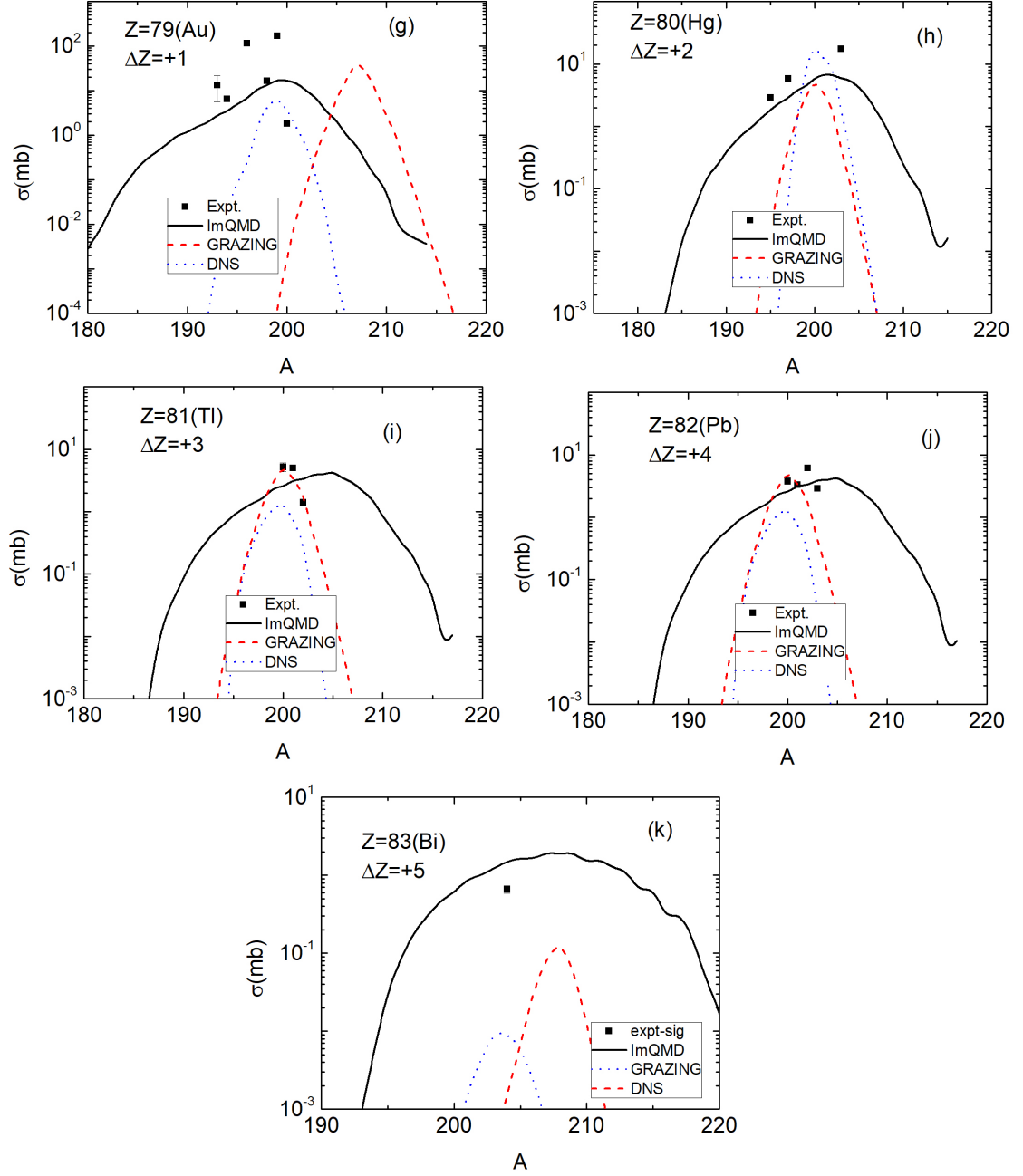


FIG. 6. Comparison of measured trans-target TLF yields (Au-Bi) to the predictions of the ImQMD, GRAZING and DNS models.

these multi-nucleon transfer reactions [11]. In Figure 7, we compare the measured mass yields, σ (A) from this work with predictions of two versions of the DNS model [9, 21]. The calculations of [9] are made for the 816 MeV $^{136}\text{Xe} + ^{198}\text{Pt}$ reaction while the calculations of [21] are made for the 708 MeV $^{136}\text{Xe} + ^{198}\text{Pt}$ reaction. Our measurements were done for the 760.5 MeV $^{136}\text{Xe} + ^{198}\text{Pt}$ reaction, so we would expect a rough agreement between the measured and predicted mass yields. Both models predict a two-humped mass distribution with yield maxima near the masses of the projectile and target nuclei. The lower energy calculation [21], predicts mass yields that are closer to the observations than the higher energy calculations [9]. Both models underestimate the near-target mass yields by orders of magnitude. A temperature dependence of the shell corrections is included in the calculations of [21] that seems to improve the predictive power of this model.

IV. CONCLUSIONS

What have we learned from this experiment? We found that: (a) The multi-nucleon transfer yields increase by an order of magnitude for the $^{136}\text{Xe} + ^{198}\text{Pt}$ reaction when the beam energy is increased from 760 MeV to 1085 MeV despite the decreased survival for the TLF nuclei. (b) The fragment mass yield distributions are two-humped as expected, but exhibit mass yields that exceed the predictions of the GRAZING and DNS models. (c) As seen with other systems, the semi-classical GRAZING model underestimates the yields of most multi-nucleon transfer products except for small transfers ($\Delta Z = 0, \pm 1$). (d) The DNS model underestimates the yields of the PLFs and most TLFs. (e) The ImQMD model adequately predicts the magnitude of the PLF and TLF yields and is superior to the GRAZING and DNS models.

We hope to improve the experimental characterization of the 760 MeV $^{136}\text{Xe} +$

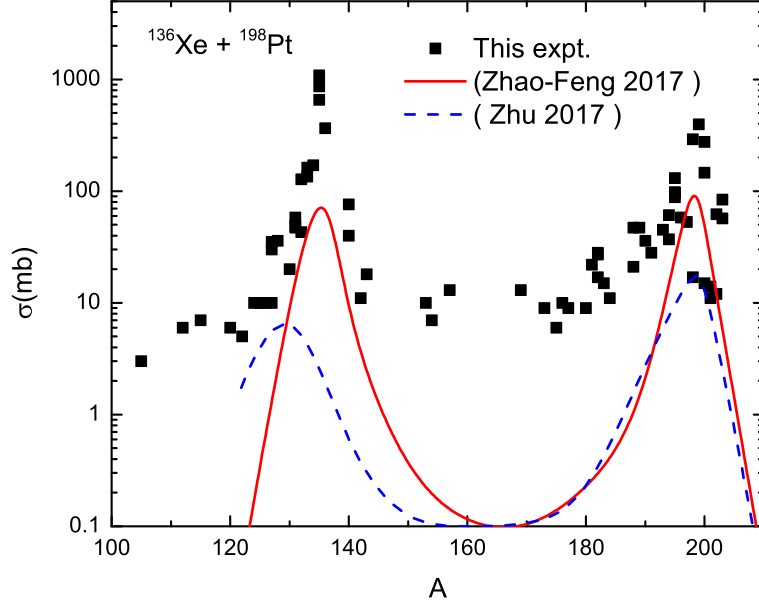


FIG. 7. Comparison of measured product mass distributions (this work) and those calculated using the two versions of the DNS model described in the text.

^{198}Pt reaction by measuring the yields of those species formed in beam in a future experiment.

V. ACKNOWLEDGMENTS

We gratefully acknowledge the effort of Prof. Feng-Shou Zhang who made the GRAZING, DNS and ImQMD calculations cited in this work. This material is based upon work supported in part by the U.S. Department of Energy, Office of Science, Office of Nuclear Physics under award numbers DE-FG06-97ER41026 (OSU), DE-FG02-97ER41041 (UNC), DE-FG02-97ER41033 (TUNL), DE-FG02-94ER40848 (UMassLowell) and contract numbers DE-AC02-06CH11357 (ANL). This research used resources of ANL's ATLAS facility, which is a DOE Office of Science User facility.

TABLE I: Projectile-like fragment and fission fragment cumulative and independent yields for $^{136}\text{Xe} + ^{198}\text{Pt}$ at $E_{cm} = 451$ MeV.

Isotope	σ_{CY} (mb)	σ_{IY} (mb)
^{43}K	0.535 ± 0.106	0.452 ± 0.090
$^{69}\text{Zn}^m$	0.0744 ± 0.048	0.0744 ± 0.048
^{72}Zn	0.287 ± 0.082	0.287 ± 0.082
^{73}Ga	2.22 ± 0.28	2.22 ± 0.28
^{72}As	0.23 ± 0.02	0.23 ± 0.02
^{97}Zr	0.36 ± 0.03	0.36 ± 0.03
^{96}Nb	0.99 ± 0.02	0.99 ± 0.02
^{99}Mo	0.81 ± 0.04	0.81 ± 0.04
$^{99}\text{Tc}^m$	0.71 ± 0.26	0.56 ± 0.21
^{105}Rh	1.26 ± 0.21	0.58 ± 0.10

Continued on next page

TABLE I – *Continued from previous page*

Isotope	σ_{CY} (mb)	σ_{IY} (mb)
^{112}Pd	1.11 ± 0.11	1.11 ± 0.11
^{110}In	1.87 ± 0.02	1.87 ± 0.02
$^{115}\text{In}^m$	2.59 ± 0.068	1.73 ± 0.45
$^{120}\text{Sb}^m$	0.374 ± 0.048	0.374 ± 0.048
^{122}Sb	1.652 ± 0.033	1.652 ± 0.033
^{126}Sb	1.42 ± 0.21	1.42 ± 0.21
^{127}Sb	2.15 ± 0.28	1.83 ± 0.24
^{128}Sb	0.82 ± 0.07	0.72 ± 0.07
$^{131}\text{Te}^m$	1.43 ± 0.31	1.43 ± 0.31
^{124}I	1.20 ± 0.05	1.20 ± 0.05
^{130}I	9.75 ± 0.04	9.75 ± 0.04
^{131}I	18.2 ± 0.5	15.3 ± 1.5
^{132}I	8.13 ± 0.29	7.97 ± 0.80
^{133}I	16.0 ± 0.1	14.6 ± 1.4
^{135}I	4.63 ± 0.42	4.63 ± 0.42
^{125}Xe	0.87 ± 0.50	0.79 ± 0.46
^{127}Xe	2.61 ± 0.43	2.24 ± 0.36
$^{133}\text{Xe}^m$	23.2 ± 0.4	21.9 ± 2.2
^{135}Xe	176 ± 1.4	164.5 ± 16.5
^{127}Cs	2.50 ± 0.78	2.31 ± 0.72
^{132}Cs	11.9 ± 0.2	11.9 ± 1.2
^{136}Cs	15.5 ± 0.4	15.5 ± 1.6

Continued on next page

TABLE I – *Continued from previous page*

Isotope	σ_{CY} (mb)	σ_{IY} (mb)
^{131}Ba	1.1 ± 0.2	0.96 ± 0.20
$^{135}\text{Ba}^m$	12.5 ± 0.2	12.5 ± 1.3
^{140}Ba	11.95 ± 0.01	10.6 ± 1.0
^{140}La	2.29 ± 0.06	2.28 ± 0.23
^{143}Ce	4.21 ± 0.08	3.56 ± 0.36
^{142}Pr	7.9 ± 2.2	7.9 ± 2.2
^{153}Sm	0.96 ± 0.20	0.78 ± 0.16
^{154}Tb	1.92 ± 0.11	1.25 ± 0.13
^{157}Dy	1.65 ± 0.09	1.39 ± 0.14
^{169}Lu	1.7 ± 1.0	1.7 ± 1.0

TABLE II: Target-like fragment cumulative and independent yields for $^{136}\text{Xe} + ^{198}\text{Pt}$ at $E_{cm} = 451$ MeV.

Isotope	σ_{CY} (mb)	σ_{IY} (mb)
^{173}Hf	0.72 ± 0.02	0.63 ± 0.06
^{175}Hf	2.51 ± 0.47	1.88 ± 0.35
$^{180}\text{Hf}^m$	0.65 ± 0.22	0.65 ± 0.22
^{176}Ta	1.35 ± 1.18	1.20 ± 1.05
^{177}Ta	2.1 ± 1.9	1.8 ± 1.6
^{184}Ta	0.82 ± 0.02	0.73 ± 0.07
^{181}Re	1.73 ± 0.78	1.53 ± 0.69
^{182}Re	8.26 ± 2.38	8.19 ± 2.43

Continued on next page

TABLE II – *Continued from previous page*

Isotope	σ_{CY} (mb)	σ_{IY} (mb)
^{188}Re	7.77 ± 0.58	7.77 ± 0.58
^{189}Re	17.5 ± 0.9	14.8 ± 1.4
^{182}Os	1.01 ± 0.16	0.95 ± 0.15
^{183}Os	0.83 ± 0.04	0.47 ± 0.05
^{188}Ir	4.28 ± 0.94	4.25 ± 0.93
^{190}Ir	3.11 ± 0.03	1.67 ± 0.17
^{194}Ir	3.18 ± 1.25	3.18 ± 1.25
$^{195}\text{Ir}^m$	17.8 ± 1.9	17.8 ± 1.9
$^{196}\text{Ir}^m$	7.57 ± 0.11	7.57 ± 0.76
^{191}Pt	5.60 ± 0.01	4.50 ± 0.45
$^{195}\text{Pt}^m$	26.5 ± 5.7	20.0 ± 4.3
^{193}Au	15.4 ± 9.0	13.4 ± 7.8
^{194}Au	6.4 ± 0.1	6.4 ± 0.6
$^{196}\text{Au}^m$	115.3 ± 0.5	115.3 ± 11.5
^{198}Au	17.6 ± 0.3	16.5 ± 1.5
^{199}Au	205.6 ± 0.6	168.8 ± 16.9
$^{200}\text{Au}^m$	1.79 ± 0.08	1.79 ± 0.18
$^{195}\text{Hg}^m$	3.4 ± 0.1	2.9 ± 0.3
^{197}Hg	6.99 ± 0.78	5.82 ± 0.65
^{203}Hg	$19.9. \pm 0.8$	$17.5. \pm 1.7$
^{200}Tl	6.2 ± 0.9	5.2 ± 0.8
^{201}Tl	6.8 ± 0.5	5.0 ± 0.5

Continued on next page

TABLE II – *Continued from previous page*

Isotope	σ_{CY} (mb)	σ_{IY} (mb)
^{202}Tl	1.4 ± 0.03	1.4 ± 0.14
^{200}Pb	4.7 ± 0.2	3.8 ± 0.4
^{201}Pb	4.4 ± 0.2	3.3 ± 0.3
$^{202}\text{Pb}^m$	6.2 ± 0.3	6.2 ± 0.6
^{203}Pb	3.9 ± 0.03	2.9 ± 0.3
^{204}Bi	0.88 ± 0.02	0.66 ± 0.07

-
- [1] V.I. Zagrebaev and W. Greiner, J. Phys. G **34**, 1 (2007)
 - [2] V. I. Zagrebaev and W. Greiner, Phys. Rev. C **83**, 044618 (2011)
 - [3] V.I. Zagrebaev and W. Greiner, Phys. Rev. Lett. **101**, 122701 (2008)
 - [4] Y.X. Watanabe, et al., Phys. Rev. Lett. **115**, 172503 (2015)
 - [5] Long Zhu, Jun Su, Wen-Jie Xie, and Feng-Shou Zhang, Phys. Lett. B **767**, 437 (2017)
 - [6] Cheng Li, Peiwei Wen, Jingjing Li, Gen Zhang, Bing Li, Xinxin Xu, Zhong Liu, Shaofei Zhu and Feng-Shou Zhang, Phys. Lett. B **776**, 278 (2018)
 - [7] Long Zhu, Pei-Wei Wen, Cheng-Jian Lin, Xiao-Jun Bao, Jun Su, Cheng Li, and Chen-Chen Guo, Phys. Rev. C **97**, 044614 (2018)
 - [8] R. Bass, Nuclear Reactions with Heavy Ions (Springer, Berlin, 1980) pp. 109-111
 - [9] Zhao-Feng, Phys. Rev. C **95**, 024615 (2017)
 - [10] A.V. Karpov and V.V. Saiko, Phys. Rev. C **96**, 024618 (2017).
 - [11] J. S. Barrett et al., Phys. Rev. C **91**, 064615 (2015)
 - [12] A. Kent, and C.A. Ungerer, private communication
 - [13] <http://www.jimfitz.demon.co.uk/fitzpeak.htm>

- [14] G. Friedlander, J.W. Kennedy, J.M. Miller, and E. Macias, Nuclear and Radiochemistry, 3rd Edition (Wiley, New York, 1981)
- [15] D.J. Morrissey, W. Loveland, M. de Saint-Simon and G.T. Seaborg, Phys. Rev. C **21**, 1783 (1980).
- [16] G. Bertsch, W. Loveland, W. Nazarewicz, and P. Talou, J. Phys. G; Nucl. Part. Phys. **42**, 077601 (2015)
- [17] <http://personalpages.to.infn.it/~nanni/grazing/>.
- [18] A. Winther, Nucl. Phys. A **572**, 191 (1994) ; A **594**, 203 (1995)
- [19] L. Corradi, G. Pollorolo, and S. Szilner, J. Phys. G: Nucl. Part. Phys. **36**, 113101 (2009)
- [20] A. Vogt et al., Phys. Rev. C **92**, 024619 (2015)
- [21] Long Zhu, Pei-Wei Wen, Cheng-Jian Lin, Xiao-Jun Bao, Jun Su, Cheng Li, and Chen-Chen Guo, Phys. Rev. C **97**, 044614 (2017)